Microrheology of cross-linked polyacrylamide networks

Bivash R. Dasgupta and D. A. Weitz
Department of Physics and DEAS, Harvard University, Cambridge, Massachusetts 02138, USA
(Received 26 August 2004; published 24 February 2005)

Experiments investigating the local viscoelastic properties of a chemically cross-linked polymer are performed on polyacrylamide solutions in the sol and the gel regimes using polystyrene beads of varying sizes and surface chemistry as probes. The thermal motions of the probes are measured to obtain the elastic and viscous moduli of the sample. Probe dynamics are measured using two different dynamic light scattering techniques, diffusing wave spectroscopy (DWS) and quasielastic light scattering (QELS) as well as video-based particle tracking. Diffusing wave spectroscopy probes the short-time dynamics of the scatterers while QELS measures the dynamics at larger times. Video-based particle tracking provides a way to investigate the local environment of the individual probe particles. A combination of all the techniques results in a larger range of frequencies that can be probed compared to conventional bulk measurements while providing local information at the level of individual probes. A modified algebraic form of the generalized Stokes-Einstein equation is used to calculate the frequency-dependent moduli. A comparison of microrheological measurements with bulk rheology exhibits striking similarity, confirming the applicability of microrheology for chemically cross-linked polymeric systems.

DOI: 10.1103/PhysRevE.71.021504 PACS number(s): 83.85.Ei, 83.85.Cg, 83.10.Pp

I. INTRODUCTION

Soft materials such as emulsions, colloidal suspensions, gels, and polymer solutions are viscoelastic in nature [1,2]; they both store and dissipate energy when responding to an external stress. These materials can be characterized by a complex shear modulus $G^*(\omega)$, which is typically measured using a rheometer, where the stress response to an applied oscillatory strain provides a measure of viscoelasticity [3]. The real part of the complex modulus, $G'(\omega)$, measures the in-phase response of the medium to an oscillatory strain and thus gives a measure of the elasticity of the material. The out-of-phase response is given by the imaginary part, $G''(\omega)$, which is related to the viscosity of the material. Recently a complementary technique called microrheology [4–20] has been developed which probes the local viscoelastic properties by measuring the response of embedded probes in the medium. Experiments have confirmed that microrheology accurately measures the elastic and viscous properties of simple systems like flexible homogeneous polymer solutions [19]. However, despite the usefulness of microrheological techniques and its applicability for simple homogeneous polymer systems, the method has still not been extensively tested for cross-linked polymeric systems to ascertain that it measures the same response of the systems as do the more conventional mechanical rheological measurements.

The addition of permanent cross-links to an otherwise flexible polymer introduces an additional length scale to the system, determined by the distance between the chemical cross-links. Both the size and the distribution of this length scale grow as the sol to gel transition is approached, and it is unclear what effect this has on the response of the probe particles. In addition, the probe particles themselves may introduce heterogeneities into the materials which may also affect their response. Unlike polymer solutions, the cross-links will prevent the network from readjusting to the presence of the probe particles, which may alter the response of the probes, and thus may lead to poorer quality response. Earlier microrheological measurements [8,21,22] on cross-linked polymer systems have explored the frequency-independent plateau shear modulus of cross-linked polyvinyl alcohol and polyacrylamide gels and have compared them with conventional bulk measurements. The laser interferometry technique used by Schnurr *et al.* [8] on polyacrylamide gels has good temporal and spatial resolution but is not designed to measure a large ensemble of beads simultaneously. The light scattering microrheological measurements done by Narita *et al.* [21] on polyvinyl alcohol compare only the frequency-independent plateau modulus with bulk rheology measurements. Detailed study of the frequency-dependent viscoelastic behavior obtained from light scattering and particle tracking measurements of cross-linked solutions and gels are required to measure the response of the polymer to the embedded probes, particularly near the sol-gel transition. These results are also important to ascertain the validity of microrheology when applied to biologically relevant materials such as actin networks [7,8,20] which also exhibit similar cross-linked architecture. Thus, it is important to determine the applicability of microrheology in chemically cross-linked systems.

The aim of this paper is to compare microrheological measurements with conventional rheological measurements for a model cross-linked polymer solution where low concentrations of probe particles are suspended. We investigate a cross-linked polymer system in both the sol and gel regimes and also near the sol-gel transition, as examples of a heterogeneous system that can provide a good test of microrheology. The frequency-dependent moduli are calculated from the probe dynamics measured using quasielastic light scattering (QELS) [23], diffusing wave spectroscopy (DWS) [24], and particle tracking measurements [25,26]. Quasielastic light scattering experiments are performed in the single scattering regime and measure the dynamics of the probe par-

ticles at larger length scales and longer time scales. By contrast, DWS measurements are made on samples in the multiple scattering regime and probe shorter length and time scales. A combination of the two techniques allows us to probe frequencies ranging from 10^{-2} to 10^{5} rad/s which is significantly larger than the range accessible with traditional rheological experiments, where the frequency range is determined primarily by inertia of the tool at high frequencies and the resolution of the transducer at low frequencies. We complement the ensemble-average light scattering measurements with video-based multiparticle tracking measurements. The use of the multiparticle tracking technique [25,26] allows us to simultaneously track about 100 probe particles in a single field of view. Using this technique we can measure the local environment of individual beads to simultaneously both obtain ensemble-averaged information and explore local heterogeneities [26]. We use both one- and two-particle [18] techniques to investigate the local and the long-wavelength response of the polymer matrix. The long-wavelength response of the polymer matrix is obtained by measuring the correlated motion of pairs of nearby beads. Two-particle measurements provide a useful tool to probe bulk properties of a material where local heterogeneities of the sample can affect one-particle measurements.

We use polyacrylamide, a chemically cross-linked polymer, as our model cross-linked system. The samples are prepared in the sol, gel, and near the sol-gel transition state by changing the cross-linker and monomer concentrations to obtain samples with different viscoelastic properties and with different characteristic length scales which are determined by the distance between the cross-links. We embed polystyrene probe particles of different size and surface chemistry to test the effect of particle size and surface properties on our microrheological measurements. A modified form of the generalized Stokes-Einstein relation is used to obtain the elastic and viscous moduli from the light scattering and particle tracking data. To check the microrheology measurements, the results of the light scattering and particle tracking measurements are compared with those obtained using a strain-controlled rheometer. We obtain excellent agreement between all our microrheology measurements and bulk rheological measurements on the same sample. This validates the use of microrheology for cross-linked polymer networks.

II. EXPERIMENTAL DETAILS

The polyacrylamide samples are prepared using a free radical polymerization reaction [27]. Acrylamide monomers (A) are mixed with N,N,N',N'-tetramethylethylenediamine, which is the initiator, and ammonium persulfate, which acts as a catalyst for the polymerization reaction. Cross-linking is achieved by adding methylenebisacrylamide (C) to the mixture. The methylenebisacrylamide molecules are essentially two acrylamide monomer units bridged by a covalent bond shown schematically by the dark lines in Fig. 1. Sol and gel phases are prepared by varying the amounts of acrylamide and methylenebisacrylamide in the sample [28]. We use 0.5 wt % of catalyst and 0.1 wt % of the initiator for all our

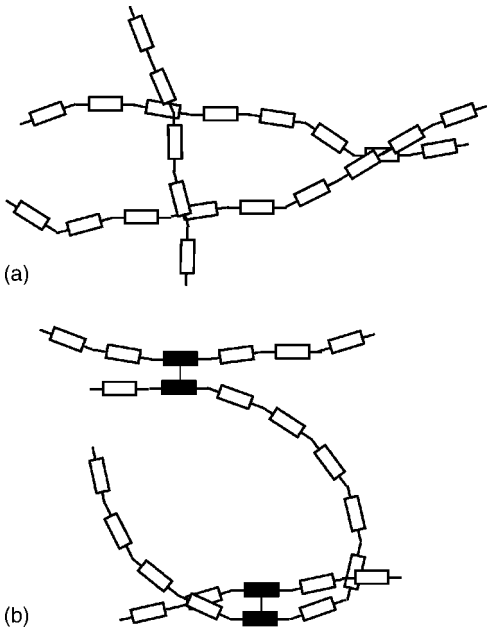

FIG. 1. (a) Acrylamide monomer units (open rectangles) are polymerized in the presence of the N,N,N',N'-tetramethylethylenediamine which is the initiator and ammonium persulfate which acts as a catalyst for the free radical polymerization reaction. (b) Cross-linking is obtained by adding methylenebisacrylamide (solid rectangles) to the mixture. The cross-linking molecules are two acrylamide monomer units bridged by a carbon atom attached to the two nitrogen atoms from two monomers.

samples. For microrheological measurements polystyrene probe particles are added to the solution before the samples are polymerized. Polymerization of the solution is monitored by measuring the absorption spectrum of the sample over time. Figure 2(a) depicts the absorption spectrum for a 3 wt % total (M+C) polyacrylamide solution with 0.05 wt % bisacrylamide taken 13 and 76 min after mixing. The decrease with time of the absorbance at 260 nm is a result of the decrease in the number of carbon-carbon double bonds due to polymerization [29] and can be used to monitor the progression of the reaction. The polymerization reaction is completed in approximately 50 min, as evidenced by the onset of the plateau in the absorption at 260 nm as a function of time, shown in Fig. 2(b). All data shown in this paper are taken 12 h to a few days after mixing the monomers and cross-linkers. We use a 3 wt % total (M+C) polymer concentration and vary the cross-linker concentration from 0.03 to 0.05 wt % to go from a gel to a sol phase. Polyacrylamide samples with 2 wt % total (M+C) polymer concentration with 0.2 wt % cross-linker concentration are prepared to investigate the response of the sample near the sol-gel transition.

Polystyrene spheres with diameters of 0.04, 0.10, 0.48, and 1.0 μm are used as probe particles. We use probe particles with different surface chemistries to investigate possible effects of surface charge of the probes. We use negatively charged carboxylate-modified (CML) and positively charged aldehyde-modified polystyrene probes. Different amounts of probe particles are added for measuring the

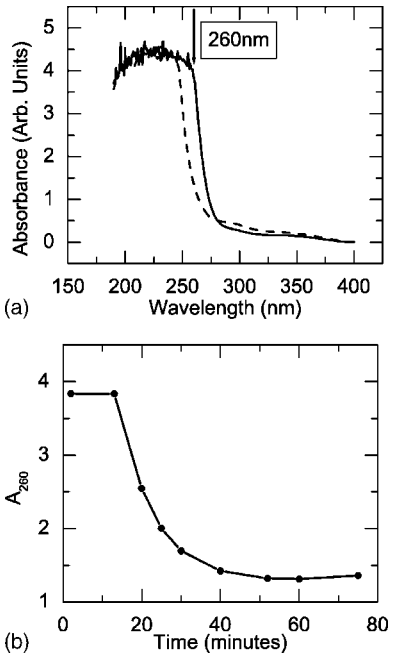

FIG. 2. (a) Absorption curves for 3 wt % polymer gel with 0.05 wt % cross-linker taken at after 13 min (solid line) and 76 min (dashed line). The decrease with time of the absorbance at 260 nm is the result of the decrease in the number of the C═C double bonds due to polymerization. (b) The filled circles denote the absorbance of the polymer solution at 260 nm, measured over time. The onset of the plateau after approximately an hour is an indication of the completion of the polymerization reaction.

sample using the three different microrheological techniques. For the video-based multiparticle tracking measurements the final bead concentration is 0.02 wt %, while for QELS measurements the final bead concentration is 0.005 wt %. A higher bead concentration is used for the multiparticle measurements to ensure a sufficient number of particles in a field of view while a lower bead concentration is used for the QELS measurements to prevent multiple scattering from affecting our results. For DWS measurements, the probe particle concentration is 1 wt % to ensure the requisite strong multiple scattering.

The dynamics of the probe particles are measured using dynamic light scattering [23,24] and video-based multiparticle tracking [25]. Dynamic light scattering provides a very good ensemble average measurement of the dynamics. We use both DWS [21,22,24] and QELS [21,23] to access a wide range of frequencies [19]. By contrast, the frequency range for multiparticle tracking microrheology is limited by the speed of the video camera [26]. However, it enables us to measure the response of the material around every probe particle, which is required to investigate local microenvironments.

Quasielastic light scattering measurements are performed on samples where embedded probe concentrations are sufficiently low that the particles scatter only once. The experiments are performed using a goniometer with a single-mode fiber optic detection system and an Ar^+ laser operating in the TEM_{00} mode with laser emission at $\lambda = 514.5$ nm (*in vacuo*). Cylindrical glass tubes with a diameter of 0.5 cm are used as sample cells. The vials are placed in a vat filled with toluene to reduce stray reflections and scattering from the vial surface. For our measurements we add polystyrene probe particles to our polymer solutions to a final concentration of ca. 0.005 wt %. This ensures that the scattering from the probe particles dominates that from the polymer solution while simultaneously limiting multiple scattering. To further reduce any remnant multiply scattered light, a polarizer, aligned parallel to the polarization of the incident beam, is placed in front of the detector. The time-averaged intensity correlation functions are collected for one to two hours at room temperature. For QELS, the electric field autocorrelation function is given by [23]

$$g_1(\tau) = e^{-q^2\langle \Delta r^2(\tau)\rangle/6}, \tag{1}$$

where $q=[4n\pi \sin(\theta/2)]/\lambda$ is the scattering vector, θ is the scattering angle, n is the refractive index of the medium, and λ is the wavelength of incident light. This is obtained from the measured intensity autocorrelation function using the Siegert relation [23]. In QELS the correlation function decays when the path length of the scattered light changes by a wavelength, which requires the individual particles to move a length that is set by the inverse of the scattering vector q. Since the scatterers have to move large distances, the characteristic decay times are larger than those obtained by diffusing wave spectroscopy.

Diffusing wave spectroscopy extends dynamic light scattering measurements to samples which are multiply scattering, using a diffusion approximation to describe the propagation of light through the sample [24]. The decay in the autocorrelation function of the multiply scattered light results from a change in the phase of the scattered light by $\sim\pi$ which is due to a change of λ in the total length of a multiply scattered light path through the sample. In DWS, the light is scattered multiple times in each path and hence each scatterer in the path needs to move only a fraction of the wavelength of the incident light. This allows us to probe motion at shorter length scales and hence faster time scales than with QELS. Diffusing wave spectroscopy measurements are done in the transmission geometry using an Ar^+ laser emitting light at $\lambda = 514.5$ nm (*in vacuo*) in the TEM_{00} mode. The beam is focused to a point on the sample cell. Glass cells (Vitrocom, NJ) with 2 mm internal thickness are used for our measurements. Multiply scattered light is depolarized, with equal intensity polarized parallel and perpendicular to the incident light. Since each polarization is independent, the signal to noise ratio is reduced and the intercept of the correlation function drops to 0.5. To circumvent this, an analyzer is used to collect only a single polarization. The scattered light is collected by an optical fiber, which is followed by a fiber-optic beam splitter connected to a pair of photomultiplier tubes. The signals from the photomultiplier tubes are cross-correlated, to circumvent the dead time of the detector electronics and reduce after-pulsing effects, allowing us to measure correlation functions at shorter delay times [23]. The correlation functions are collected for 1–2 h at room temperature. In DWS, all scattering-vector information is lost; as a result, only two experimental geometries, trans-

mission and backscattering, are used. The field autocorrelation function at a delay time τ is [24]

$$g_1(\tau) \propto \int_0^\infty P(s)\exp\left[-k_0^2\langle\Delta r^2(\tau)\rangle\frac{s}{3l^*}\right]ds, \qquad (2)$$

where $P(s)$ is the probability of light traveling a path of length s, and is determined by solving the diffusion equation for the propagation of light for the relevant geometry and with the correct boundary conditions, and $k_0=2n\pi/\lambda$ is the wave vector of the incident light. The transport mean free path of the light, l^*, is a characteristic of the sample itself and reflects the length the light must travel before its direction is randomized. To ensure sufficiently strong multiple scattering, the transport mean free paths for all the samples used in these experiments are adjusted to be at least five times smaller than the cell thickness. The transport mean free path of each sample is obtained by measuring the ratio of the intensity of the light transmitted through the sample to that transmitted through a reference sample whose value of l^* is known, using identical optical geometries [19,24].

When the signals are ergodic, the time-averaged intensity correlation function $g_2(\tau)$ is measured and the field correlation function is obtained using the Siegert relation [23] for both QELS and DWS experiments. However, for many of the gel samples, the signal is no longer ergodic; and the time-averaged correlation functions do not represent true ensemble-averaged data. In these cases, we employ an averaging technique [30] to obtain the true ensemble-averaged correlation function from the measured data. The mean square displacement $\langle\Delta r^2(\tau)\rangle$ for quasielastic light scattering measurements is calculated from Eq. (1) above. In the case of diffusing wave spectroscopy measurements, the mean square displacement is calculated by using the measured mean free path and numerically inverting the field correlation function shown in Eq. (2).

To prepare the samples for the multiparticle tracking measurements, we mix the monomers, initiator, catalyst, and probe particles in desired proportions. The mixed solutions are immediately loaded into glass microscope sample chambers consisting of three 1 mm thick glass spacers sandwiched between a glass slide and a no. 1.5 glass cover slip. The glass is cleaned using a mixture of filtered water and methanol, and the sample cell is assembled and sealed with optical grade glue which can be cured using ultraviolet light. Once loaded, the chamber is sealed using the same uv-curing glue and the sample is allowed to polymerize for 6 h at room temperature. After the polymerization is complete, the particles are imaged with an inverted research microscope (Leica DM-IRB) using bright-field illumination or epifluorescence depending on the type of polystyrene probes used. Images are captured using a charge-coupled device camera (COHU Electronics) at frame rates of 30 Hz for 3–10 min and are directly digitized in real time using software custom written for image analysis [25]. The positions of the beads in each frame are identified by finding the brightness-averaged centroid of each bead, which is determined with a resolution of 20–30 nm; these are then linked together to form time tracks of each probe particle. The particle tracks are used to calculate the ensemble-averaged mean square displacements [25]. The highest frequency accessible using this technique is determined by the frame rate of the camera, while the lowest frequency is determined by the maximum measurement time which is typically a few minutes. Thus the angular frequency range accessible with video-based particle tracking is between 0.1 and approximately 10 rad/s; this is less than the range accessible using light scattering techniques. However, using multiparticle tracking, we can measure the local environment of a single probe as well as the longer wavelength response of the material which is probed by measuring the correlated motion of pairs of nearby beads [18]. The correlated motion of the beads directly reflects the propagation of the strain field through the sample; this decays as the inverse of the distance between them. Hence, the correlated mean square deviation (MSD) is immune to local heterogeneities and probes the macroscopic response of the system. The two-particle distinct MSD $\langle\Delta r^2(\tau)\rangle_D$ is defined as [18]

$$\langle\Delta r^2(\tau)\rangle_D = \frac{2r}{a}D_{rr}(r,\tau), \qquad (3)$$

where a is the bead radius and D_{rr} is the ensemble-averaged two-particle displacement correlation tensor, which is calculated as [18]

$$D_{\alpha\beta}(r,\tau) = \langle\Delta r_\alpha^i(t,\tau)\Delta r_\beta^j(t,\tau)\,\delta(r-R^{ij}(t))\rangle_{i\neq j,t}, \qquad (4)$$

where Δr_α^i is the displacement of the ith particle in the α component of the direction, i and j label different particles, α and β label different coordinates, and $R^{ij}(t)$ is the distance between the particles i and j. The averaging is done over the distinct terms $(i\neq j)$. This two-particle method is independent of the size of the probe used to measure the response of the system.

The MSD data obtained from the light scattering and particle tracking experiments are converted to elastic and viscous moduli using a modified algebraic form [18,19] of the generalized Stokes-Einstein equations [14,17]:

$$G'(\omega) = G(\omega)\{1/[1+\beta'(\omega)]\}\cos\left[\frac{\pi}{2}\alpha'(\omega) - \beta'(\omega)\alpha'(\omega)\left(\frac{\pi}{2}-1\right)\right],$$

$$G''(\omega) = G(\omega)\{1/[1+\beta'(\omega)]\}\sin\left[\frac{\pi}{2}\alpha'(\omega) - \beta'(\omega)[1-\alpha'(\omega)]\left(\frac{\pi}{2}-1\right)\right], \qquad (5)$$

where

$$G(\omega) = \frac{k_BT}{\pi a\langle\Delta r^2(1/\omega)\rangle\Gamma(1+\alpha(\omega))[1+\beta(\omega)/2]}. \qquad (6)$$

The first- and second-order logarithmic time derivatives of the MSD data are denoted by $\alpha(\omega)$ and $\beta(\omega)$, respectively, while $\alpha'(\omega)$ and $\beta'(\omega)$ denote the local first- and second-order logarithmic derivatives of $G(\omega)$, respectively. A second-order polynomial fit using a sliding Gaussian window

is used to numerically calculate the local first- and second-order logarithmic derivatives and to smooth the data. We use Eq. (6) to obtain $G(\omega)$ from the MSD data using the above procedure. We then use the remaining two equations given in Eq. (5) and repeat the local power law fitting on $G(\omega)$ to obtain the elastic and loss moduli. This method of analysis avoids numerical transformations of our data or the need to use functional forms to fit the modulus in Laplace frequency space.

To ascertain the heterogeneity of the polyacrylamide samples we can measure the distribution of displacements [26] of all the beads in our field of view. For a homogeneous sample the individual probes will explore a similar environment and the distribution will be Gaussian; their widths will reflect the local response of the system. By contrast, probes in a heterogeneous environment will experience a different local environment each of which can result in Gaussian distributions of displacements whose widths reflect the different local environments. However, an ensemble average of the distribution of all the beads will result in a non-Gaussian distribution.

Rheological measurements are performed to compare microrheology with traditional bulk rheology. We measure the frequency-dependent elastic modulus $G'(\omega)$ and viscous modulus $G''(\omega)$ of our samples with a strain-controlled rheometer using a double-wall Couette geometry for all the polyacrylamide samples. We compare polymer samples in both the presence and absence of the probe particles. Since the gels are irreversible the samples are prepared *in situ* at room temperature in the rheometer. Strain sweeps, where the elastic, $G'(\omega)$, and the viscous, $G''(\omega)$, moduli are plotted as a function of the maximum applied strain, are performed at different frequencies ranging from 0.5 to 50 rad/s to determine the linear region of measurement of the moduli for the polymer solutions. All subsequent measurements of the frequency dependence of the storage and loss moduli are performed at strains sufficiently low to ensure linear response.

III. RESULTS

The scaled mean square displacements measured using particle tracking techniques for two probe sizes embedded in a "sol" sample where the total polyacrylamide concentration is 3 wt % and the cross-linker concentration is 0.03 wt % are shown in Fig. 3. The scaled MSD's of 0.48 and 1.0 μm diameter probe particles are shown by the solid and dashed lines, respectively. The MSD's are scaled with the bead radius to provide an indication of any bead size dependence in the behavior of probed particles in the cross-linked polymer solutions. Both data sets scale together, indicating the independence of the probe size when measuring the moduli of the material. The open symbols represent the two-particle-correlated MSD's, again scaled by the bead size. Both the one- and two-particle MSD's overlap with each other which indicates that the material is homogeneous at these length scales.

The polymer backbone, which contains aminocarbonyl (—$CONH_2$) groups, can undergo hydrolysis and form carboxyl (—COOH) groups, which can dissociate in an aqueous environment to leave the backbone with a very weak negative charge. This might lead to specific adsorption onto the surface of the probe particles, which are themselves charged, and could modify the measured results. To check for this possibility, we compare polystyrene probe particles of the same size, but with different surface chemistries. We use 1.0 μm diameter polystyrene probe particles with positively charged aldehyde-amidine- and negatively charged carboxylate-modified surfaces. A plot of the MSD's measured using DWS for 1 wt % probe particles dispersed in a 3 wt % polyacrylamide "gel" sample with 0.05 wt % cross-linker concentration is shown in Fig. 4. The open circles denote the results obtained using the positively charged aldehyde-amidine particles while the solid line denotes those obtained with the negatively charged CML probe particles. Because these samples are nonergodic, we average [30] the correlation functions to obtain the true ensemble average. The correlation functions are converted to mean square displacements and are plotted in Fig. 4. The mean square dis-

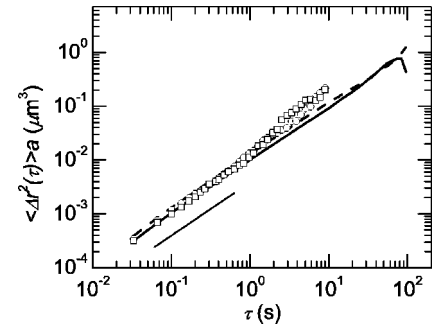

FIG. 3. Plot of the scaled mean square displacements of probe particles measured by using multiparticle tracking in a 3 wt % total polyacrylamide sample with 0.03 wt % cross-linker concentration. The MSD's are scaled with the corresponding probe sizes. The one-particle MSD for 0.48 μm (solid line) polystyrene spheres overlaps with that of the 1.0 μm (dashed line) particles. The scaled two-particle MSD's for 0.48 μm (circles) and 1.0 μm (squares) show good agreement with each other and with the one-particle MSD. The line indicates a slope of 1.

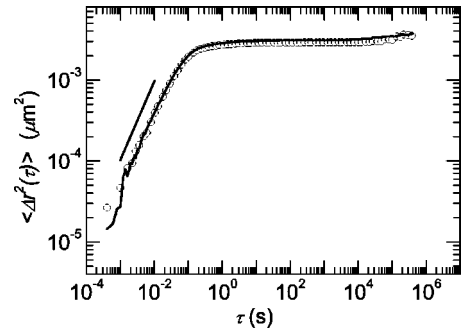

FIG. 4. Effect of different bead chemistry. Comparison of the mean square displacements probed with 1.0 μm negatively charged carboxylate-modified (solid line) and positively charged aldehyde-amidine (circles) polystyrene spheres in a 3 wt % total polyacrylamide gel sample with 0.05 wt % cross-linker concentration. The excellent overlap of the data suggests that there is not a significant effect due to the surface chemistry of these probe particles.

placements have slopes near 1 at short time scales indicating predominantly viscouslike behavior while at longer time scales the slopes are closer to 0 reflecting an elastic response as expected for gelled samples. The mean square displacements for the two types of probes overlap very well with each other, indicating that the bead surface chemistry does not affect our measurements.

Polyacrylamide is known to be a heterogeneous polymer [31]; the addition of cross-links results in a broad distribution of mesh sizes which can vary depending on whether the sample is a sol or a gel. To probe the heterogeneity of the polymer, particle tracking measurements are performed on a polyacrylamide "gel" with 3 wt % polymer and 0.05 wt % cross-linker concentration using rhodamine-dyed 40 nm diameter polystyrene particles as probe particles. Although the ensemble-averaged response provides a measure of the average macroscopic response of the material, individual probe particle measurements are necessary to characterize the microenvironments. The MSD's of many individual probe particles suspended in the sample are shown in Fig. 5(a) where large variations in the MSD's of the different particles are observed. Although it is very tempting to ascribe the wide distribution of the MSD's to spatial heterogeneities present in our sample, which could be due to different local elasticity or to differences in the local structure of the gel, we are limited by the fact that the individual probe particle data are not sufficiently time averaged to provide an appropriate measure of the heterogeneity. In order to better distinguish the effects of insufficient statistics from true sample variations [26], we plot the probability distribution $P(\Delta x)$ of the displacements Δx at a fixed lag time Δt of all the beads in the field of view. These distributions provide better evidence of the heterogeneity of the samples since we can compare both the individual probe particle and the ensemble-averaged distributions. The probability distributions of displacements of two individual particles at a lag time of 0.1 s are shown in Fig. 5(b); both distributions can be fitted to a Gaussian, but with different widths. By contrast, the probability distribution of individual particles embedded in a homogeneous material can be fitted to a Gaussian with the same width [26]. For a purely homogeneous material the ensemble-averaged probability distribution of the probe displacements is Gaussian [26]. However, the ensemble-averaged distributions for the polyacrylamide gel are non-Gaussian at large displacements when calculated at lag times of 0.033 and 0.1 s and plotted using diamonds and triangles, respectively, in Fig. 5(c). The non-Gaussian nature of the probability distribution of displacements, as seen in the tails of the distribution functions, is due to the averaging of individual distribution functions of different widths; the different widths in the distribution signify different local environments for the probes which result from the heterogeneous nature of the polyacrylamide sample.

Rheological measurements are performed to compare with microrheological measurements of the polymer solutions and gels. Most of the measurements are done in the absence of probe particles at room temperature and the samples are mixed in the tool itself to avoid breakage of the network, which might occur while loading gelled samples in the tool. Separate experiments confirm that the presence of probe particles does not affect the bulk rheological measurements; this is accomplished by comparing the results for 3 wt % polyacrylamide solutions with 0.03 and 0.05 wt % cross-linker concentration with 0.02 wt % 1 μm diameter

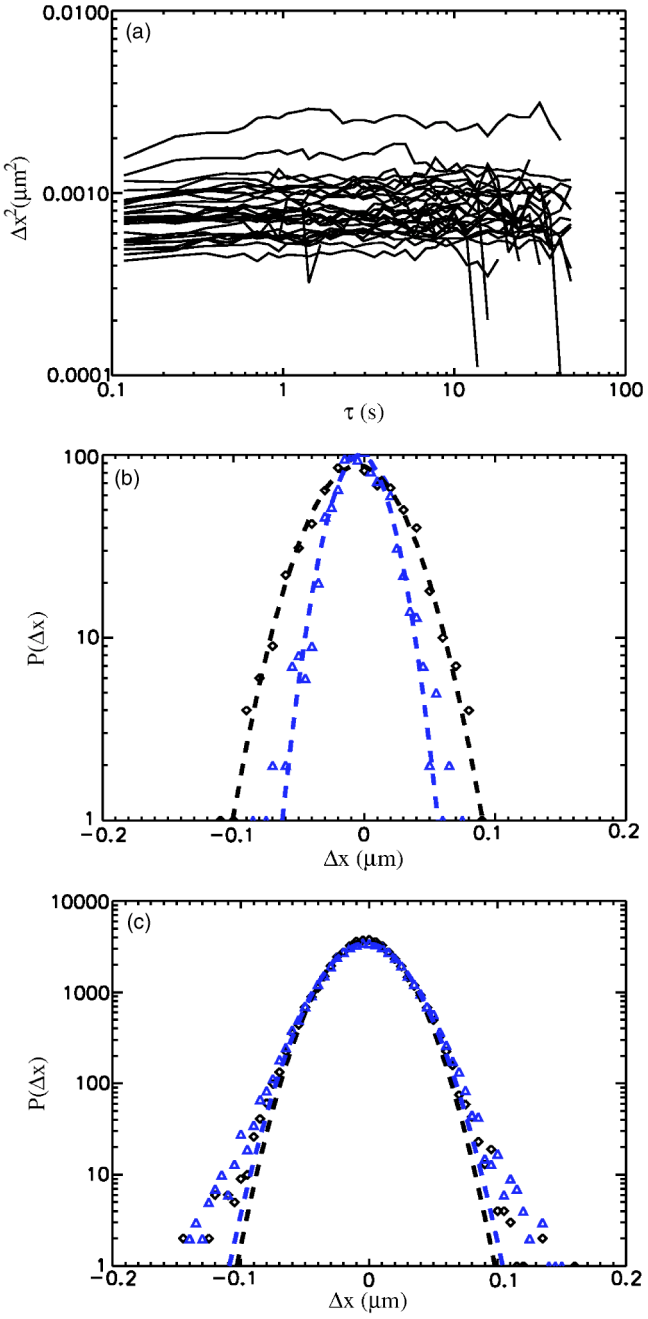

FIG. 5. (Color online) Measure of heterogeneity in the polyacrylamide samples. Van Hove correlation functions for 0.1 μm diameter particles moving in a 3 wt % total polyacrylamide solution with 0.05 wt % cross-linker concentration. (a) The spread of the individual particle mean square displacements for several particles is an indicator of the difference in local elasticity measured by the probes. (b) Individual particle distributions, shown at a time lag of 0.1 s, are each well described by a Gaussian, albeit of different widths indicating different local environments. (c) The ensemble-averaged distributions, shown at time lags of 0.033 s (diamonds) and 0.1 s (triangles) are non-Gaussian at large displacements.

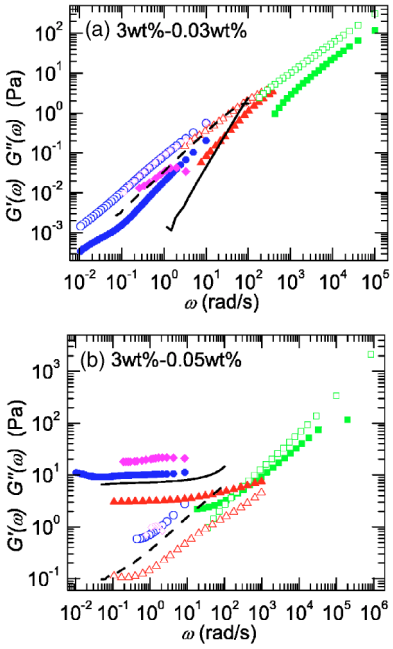

FIG. 6. (Color online) Comparison of the storage and loss moduli for a sol (a) and a gel (b) sample obtained from bulk rheology (G', solid line; G'', dashed line) with diffusing wave spectroscopy (DWS) [(green) squares], quasielastic light scattering (QELS) [(red) triangles], and one-particle [(blue) circles] and two-particle [(magenta) diamonds] microrheology measurements. The solid and open symbols denote the storage and the loss moduli, respectively. For microrheology measurements every third data point is plotted for clarity.

polystyrene probe particles with similar polymer solutions without probe particles.

Microrheological measurements obtained from QELS, DWS, and particle tracking experiments on polyacrylamide samples are compared directly with bulk rheological measurements and are shown in Fig. 6. The comparison for "sol" and "gel" samples are shown in Figs. 6(a) and 6(b), respectively, where the symbols denote data obtained from microrheological techniques and the lines denote data obtained from bulk rheological measurements. For all the microrheology measurements every third data point is plotted for clarity. The modified algebraic form of the generalized Stokes-Einstein equations given in Eqs. (5) and (6) is used to calculate the elastic and viscous moduli from MSD's obtained from light scattering and particle tracking measurements. A combination of all these different microrheological methods enables us to probe almost eight decades in frequency, which is considerably larger than the frequency range accessible by any one technique or by bulk rheological measurements.

We use 0.48 μm diameter polystyrene spheres for all microrheology measurements performed on a "sol" sample which is prepared using 3 wt % total polyacrylamide and 0.03 wt % cross-linker. As expected for a sol, the viscous modulus shown using open symbols dominates over the elastic modulus which is plotted using filled symbols, indicating that the sample is a viscoelastic fluid over the entire range of frequencies investigated. The slope of the viscous moduli changes from close to 0.9 in the low-frequency regime to 0.75 at the higher frequencies, indicating a change in the response of the sample from a viscouslike behavior to a comparatively more elasticlike behavior. The viscous modulus obtained from the one- and two-particle microrheological measurements, shown using circles and diamonds, respectively, overlap with each other, indicating a homogeneous sample. The viscous modulus obtained from single scattering measurements, shown using triangles, compares very well both with the multiparticle tracking measurements and with the DWS measurements, which are shown using open squares. The viscous modulus obtained from bulk rheological measurement, shown by the dashed line, is in better agreement with QELS- and DWS-based microrheological methods than with the low-frequency particle tracking measurements, but the differences are relatively small. Although the dominant viscous modulus obtained from the different techniques overlaps very well, the comparison for the elastic modulus is not as good; this is typical of the subdominant modulus in microrheological experiments.

The comparison of moduli obtained from microrheological and rheological experiments performed on a 3 wt % total polyacrylamide with 0.05 wt % cross-linked "gel" is shown in Fig. 6(b). For particle tracking measurements on this sample we use 0.1 μm diameter rhodamine-dyed probe particles while the light scattering measurements are done using 0.48 μm diameter carboxylate modified polystyrene probe particles. The gel sample exhibits a dominant elastic plateau with significantly lower viscous modulus at low frequencies while at higher frequencies both the elastic and loss moduli are comparable. At very short lag times the polymer chains are free to diffuse around which results in a more viscouslike response at high frequencies. However, at longer times these chains are constrained in their excursions due to the cross-links of the polymer matrix, resulting in the frequency-independent plateau at low frequencies. Using DWS, we are able to probe the shorter time or higher-frequency regime where the moduli are comparable; the data are plotted as squares. By contrast, QELS and one- and two-particle tracking measurements, shown using triangles, circles, and diamonds, respectively, probe the low-frequency plateau regime very well. The elastic modulus obtained from microrheological measurements using QELS and DWS compares very well in the region of overlap between 10 and 1000 rad/s. The viscous modulus obtained from these techniques also compares very well. Elastic and viscous moduli obtained using particle tracking are however slightly larger than the moduli obtained from DWS and QELS measurements. Elastic and viscous moduli obtained from bulk rheological measurements exhibit features which are very similar to the low-frequency behavior obtained from the microrheological measurements using QELS and particle tracking where a predominantly elastic plateau is observed. The variation in the plateau elastic modulus values, ~3 Pa for QELS and ~10 Pa for particle tracking, is due to the sample-to-sample variation in the preparation of the gel and has also been observed in the bulk rheological measurements. Oxygen from the atmosphere can react with the unpolymerized monomers and prevent the polymerization of those monomers. This affects the rigidity of the gels due to a lower

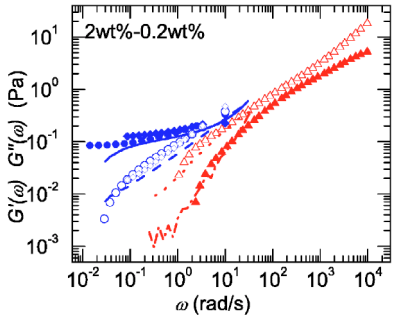

FIG. 7. (Color online) Moduli for 2 wt % total polyacrylamide solution with 0.2 wt % cross-linker concentration, which is near the sol-gel transition. Bulk rheology data measured on two separately prepared samples denoted by different line styles are compared with QELS (triangles) and one-particle (circles), and two-particle (diamonds) microrheology measurements. The solid and open symbols denote the storage and the loss moduli, respectively. The bulk data on one sample (G', solid line; G'', dashed line) show a dominant elastic modulus. By contrast, an identical sample prepared on a different day (G', dot-dashed line; G'', dotted line) with the same concentration shows a more viscouslike response for the same frequency interval. Both these data compare very well to microrheological measurements which are done using different techniques and where the samples are prepared separately. Every third data point is plotted for the microrheological measurements for purposes of clarity.

number of acrylamide and bis-acrylamide monomers in the polymer matrix, resulting in the sample-to-sample variation in the moduli. We conclude that, using different microrheological techniques, we are able to measure the same response as those obtained by bulk rheological measurements for both a cross-linked "sol" and a "gel" polyacrylamide sample.

The cross-linkers of the polyacrylamide samples introduce an additional length scale in the system which is determined by the distance between the cross-links. Both the size and the distribution of this length scale grow as the sol to gel transition is approached, and it is unclear what effect this has on the response of the probe particles. To investigate this effect, microrheological and rheological measurements are performed on a polyacrylamide sample close to the sol-gel transition. We use 2 wt % total polymer and 0.2 wt % *bis*-acrylamide sample and compare the elastic and viscous moduli obtained from a rheometer to those obtained from QELS and particle tracking microrheological techniques. Microrheological measurements obtained from one- and two-particle tracking measurements are shown by circles and diamonds while results obtained from QELS measurements are plotted using triangles in Fig. 7. For each of the microrheological measurements the elastic and viscous moduli are plotted using filled and open symbols, respectively. Since the sample is very close to the gel transition line small differences in the monomer and cross-linker concentrations can result in vastly different behavior as a result of the sample being either in the sol or in the gel state. This is experimentally observed in our microrheological measurements where the response obtained from QELS measurements exhibits predominantly viscouslike behavior while that obtained from particle tracking measurements exhibits a dominant elastic nature. Rheological measurements performed on two samples with similar polymer concentrations also exhibit similar variations in the moduli. The solid and dashed lines in Fig. 7 denote elastic and viscous moduli of one sample where the elastic modulus dominates while the dot-dashed and dotted lines denote the elastic and viscous moduli for the other sample where the viscous modulus dominates. The microrheological techniques exhibit similar variations in the moduli when compared to those obtained from bulk measurements for a cross-linked sample very near the transition.

Our results confirm that QELS, DWS, and particle tracking microrheological techniques can be successfully used to measure the elastic and viscous moduli of cross-linked polymer solutions. The dominant viscous modulus for a "sol" sample obtained from microrheological techniques compare very well with that obtained from the bulk rheological measurements. Likewise, for the "gel" sample the elastic modulus measured using the various techniques exhibit a similar plateau modulus. Furthermore, the use of DWS-based microrheology allows us to probe higher frequencies where a more viscouslike regime is observed for the gel samples. The ability to measure this marked difference in the frequency-dependent response of the gel is possible because of the multitude of microrheological techniques available to us. Particle tracking measurements confirm the heterogeneity of the polymer matrix; however, sample-to-sample variations in the preparation of the polymer samples are much larger than the measured heterogeneities. Our results show that the viscoelastic response is independent of the size and surface chemistry of the probe particles and we can conclude that the probe particles do not introduce any further heterogeneity in the system.

IV. CONCLUSIONS

We show that quasielastic light scattering, diffusing wave spectroscopy, and video-based particle tracking techniques can be used to measure the viscoelastic properties of a chemically cross-linked polymer. The use of diffusing wave spectroscopy and quasielastic light scattering enables us to probe almost eight decades in frequency which is not available using traditional bulk measurements using a rheometer. In the frequency regime where all the measurements overlap, the elastic and loss moduli obtained from the different microrheological techniques agree well with rheological measurements for both the sol and gel states of the chemically cross-linked polymer. Microrheological and rheological measurements performed on samples near the sol-gel transition exhibit similar variations in the elastic and viscous moduli. We conclude that our experiments validate the ability of microrheology for studying permanently cross-linked polymeric systems.

ACKNOWLEDGMENTS

The authors would like to thank M. Gardel and M. T. Valentine for useful discussions. B.R.D. would like to thank Johan Mattsson for reading the manuscript. This work was supported by NSF Grant No. (DMR-0243715).

[1] C. W. Macosko, *Rheology: Principles, Measurements and Applications* (VCH, New York, 1994).
[2] R. G. Larson, *The Structure and Rheology of Complex Fluids* (Oxford University Press, New York, 1999).
[3] J. D. Ferry, *Viscoelastic Properties of Polymers* (Wiley, New York, 1980).
[4] F. Ziemann, J. Rädler, and E. Sackmann, Biophys. J. **66**, 2210 (1994).
[5] F. Amblard, B. Yurke, A. N. Pargellis, and S. Leibler, Rev. Sci. Instrum. **67**, 818 (1996).
[6] F. G. Schmidt, F. Ziemann, and E. Sackmann, Eur. Biophys. J. **24**, 348 (1996).
[7] F. Gittes, B. Schnurr, P. D. Olmsted, F. C. MacKintosh, and C. F. Schmidt, Phys. Rev. Lett. **79**, 3286 (1997).
[8] B. Schnurr, F. Gittes, F. C. MacKintosh, and C. F. Schmidt, Macromolecules **30**, 7781 (1997).
[9] L. A. Hough and H. D. Ou-Yang, J. Nanopart. Res. **1**, 495 (1999).
[10] D. Velegol and F. Lanni, Biophys. J. **81**, 1786 (2001).
[11] N. J. Tao, S. M. Lindsay, and S. Lees, Biophys. J. **63**, 1165 (1992).
[12] M. Radmacher, M. Fritz, and P. K. Hansma, Biophys. J. **69**, 264 (1995).
[13] R. E. Mahaffy, C. K. Shih, F. C. MacKintosh, and J. Käs, Phys. Rev. Lett. **85**, 880 (2000).
[14] T. G. Mason and D. A. Weitz, Phys. Rev. Lett. **74**, 1250 (1995).
[15] T. Gisler and D. A. Weitz, Curr. Opin. Colloid Interface Sci. **3**, 586 (1998).
[16] A. Palmer, T. G. Mason, J. Xu, S. C. Kuo, and D. Wirtz, Biophys. J. **76**, 1063 (1999); A. Palmer, J. Xu, and D. Wirtz, Rheol. Acta **37**, 97 (1998).
[17] T. G. Mason, Rheol. Acta **39**, 371 (2000); T. G. Mason, K. Ganesan, J. H. van Zanten, D. Wirtz, and S. C. Kuo, Phys. Rev. Lett. **79**, 3282 (1997).
[18] John C. Crocker, M. T. Valentine, Eric R. Weeks, T. Gisler, P. D. Kaplan, A. G. Yodh, and D. A. Weitz, Phys. Rev. Lett. **85**, 888 (2000).
[19] B. R. Dasgupta, S.-Y. Tee, J. C. Crocker, B. J. Frisken, and D. A. Weitz, Phys. Rev. E **65**, 051505 (2002).
[20] M. L. Gardel, M. T. Valentine, J. C. Crocker, A. R. Bausch, and D. A. Weitz, Phys. Rev. Lett. **91**, 158302 (2003).
[21] T. Narita, A. Knaebel, J.-P. Munch, and S. J. Candau, Macromolecules **34**, 8224 (2001).
[22] G. Nisato, P. Hebraud, J.-P. Munch, and S. J. Candau, Phys. Rev. E **61**, 2879 (2000).
[23] B. J. Berne and R. Pecora, *Dynamic Light Scattering: With Applications to Chemistry, Biology and Physics* (Wiley, New York, 1976).
[24] D. J. Pine, D. A. Weitz, P. M. Chaikin, and E. Herbolzheimer, Phys. Rev. Lett. **60**, 1134 (1988); D. A. Weitz and D. J. Pine, in *Dynamic Light Scattering*, edited by W. Brown (Oxford University Press, Oxford, 1992); G. Maret and P. E. Wolf, Z. Phys. B: Condens. Matter **65**, 409 (1987).
[25] J. C. Crocker and D. G. Grier, J. Colloid Interface Sci. **179**, 298 (1996).
[26] M. T. Valentine, P. D. Kaplan, D. Thota, J. C. Crocker, T. Gisler, R. K. Prud'homme, M. Beck, and D. A. Weitz, Phys. Rev. E **64**, 061506 (2001).
[27] P. J. Flory, *Principles of Polymer Chemistry* (Cornell University Press, Ithaca, NY, 1953).
[28] R. Bansil and M. K. Gupta, Ferroelectrics **30**, 63 (1980); I. Nishio, J. C. Reina, and R. Bansil, Phys. Rev. Lett. **59**, 684 (1987).
[29] Bio-Rad Laboratories Bulletin 1156 (unpublished).
[30] J. G. H. Joosten, E. T. F. Gelade, and P. N. Pusey, Phys. Rev. A **42**, 2161 (1990); P. N. Pusey and W. Van Megen, Physica A **157**, 705 (1989).
[31] T.-P. Hsu and C. Cohen, Polymer **25**, 1419 (1984); A. M. Hecht, R. Duplessix, and E. Geissler, Macromolecules **18**, 2167 (1985).